Journal of Computational Neuroscience 3, 347–368 (1996)

The Use of System Identification Techniques in the Analysis of Oculomotor Burst Neuron Spike Train Dynamics

KATHLEEN E. CULLEN
Aerospace Medical Research Unit, McGill University, Montreal Quebec H3G 1Y6, Canada
Cullen@medcor.McGill.ca

CLAUDIO G. REY AND DANIEL GUITTON
Montreal Neurological Institute, McGill University, Montreal Quebec H3G 1Y6, Canada

HENRIETTA L. GALIANA
Department of Biomedical Engineering, McGill University, Montreal Quebec H3G 1Y6, Canada

Received February 7, 1995; Revised June 12, 1996

Action Editor: Barry Richmond

Abstract. The objective of system identification methods is to construct a mathematical model of a dynamical system in order to describe adequately the input-output relationship observed in that system. Over the past several decades, mathematical models have been employed frequently in the oculomotor field, and their use has contributed greatly to our understanding of how information flows through the implicated brain regions. However, the existing analyses of oculomotor neural discharges have not taken advantage of the power of optimization algorithms that have been developed for system identification purposes. In this article, we employ these techniques to specifically investigate the "burst generator" in the brainstem that drives saccadic eye movements. The discharge characteristics of a specific class of neurons, inhibitory burst neurons (IBNs) that project monosynaptically to ocular motoneurons, are examined. The discharges of IBNs are analyzed using different linear and nonlinear equations that express a neuron's firing frequency and history (i.e., the derivative of frequency), in terms of quantities that describe a saccade trajectory, such as eye position, velocity, and acceleration. The variance accounted for by each equation can be compared to choose the optimal model. The methods we present allow optimization across multiple saccade trajectories simultaneously. We are able to investigate objectively how well a specific equation predicts a neuron's discharge pattern as well as whether increasing the complexity of a model is justifiable. In addition, we demonstrate that these techniques can be used both to provide an objective estimate of a neuron's dynamic latency and to test whether a neuron's initial firing rate (expressed as an initial condition) is a function of a quantity describing a saccade trajectory (such as initial eye position).

Keywords: oculomotor, burst neurons, system identification, saccade, modeling

1. Introduction

The use of mathematical models to study the flow of neural signals in the complex circuitry of the oculomotor system is a well established procedure. However, the analyses of oculomotor neural discharges so far published have not taken advantage of the power of optimization algorithms developed for system

identification purposes. In this article, analysis techniques as well as the usefulness and power of the algorithms will be illustrated by analyzing the discharge characteristics of two typical neurons belonging to a class of cells called inhibitory burst neurons (IBNs). IBNs, along with excitatory burst neurons (EBNs), are monosynaptically connected to, respectively, antagonist and agonist motoneurons that innervate extraocular muscles. Together IBNs and EBNs are thought to provide the principal drive onto these cells during the rapid movements of the eyes called *saccades* (Hikosaka and Kawakami, 1977; Hikosaka et al., 1978; Igusa et al., 1980; Sasaki and Shimazu, 1981; Scudder, 1988; Strassman et al., 1986a, 1986b; Yoshida et al., 1982). The algorithm we present is based on the previous work of Rey and Galiana (1993) in which they described a novel method for analyzing vestibular nystagmus. The algorithm presented here allows for optimization across multiple eye trajectories simultaneously and has provided us with a new method of objectively investigating: (1) a burst neuron's dynamic latency, (2) how well a given model predicts a neuron's discharge pattern, (3) whether increasing the complexity of a model is justifiable, and (4) the relationship between initial conditions and quantities describing the saccades' trajectories.

We based our analysis of IBN firing rate on physiological models such as the one described in Fig. 1A (Jurgens et al., 1981), which is a modification to the original Robinson model (1975). Such a model predicts that burst neuron firing rate is related simultaneously "upstream" to a motor error signal $\varepsilon(t) = \Delta T - \Delta E^*$, where ΔT is desired saccade amplitude and ΔE^* is the angle the eye has turned and "downstream" to the dynamics of the saccade. In this study, to illustrate our approach, we have concentrated on estimating IBN activity based on downstream signals. Specifically, we postulate different linear and nonlinear dynamic black-box models that predict IBN firing rate based on properties of the eye's trajectory and burst history (Fig. 1B).

For didactic purposes, the oculomotor plant can be approximated as a simple first-order visco-elastic system (Robinson, 1970; see Fuchs et al., 1985, for a review). In this simplified view motoneural firing rate is written as

$$\mathrm{MN}(t) = r + kE(t - t_d) + b\dot{E}(t - t_d), \qquad (1)$$

where $\mathrm{MN}(t)$ is neural firing rate, k and b are constants, r is a bias term, E and $\dot{E}$ are eye position and velocity, respectively, and t_d is a delay. During rapid eye movements (saccades), viscous forces dominate plant dynamics, and the motoneuron discharge has been further simplified as $\mathrm{MN}(t) \propto \dot{E}(t - t_d)$ (Robinson, 1964). Consistent with the view that burst neurons monosynaptically excite motoneurons, the dynamics of burst neuron discharges have also been

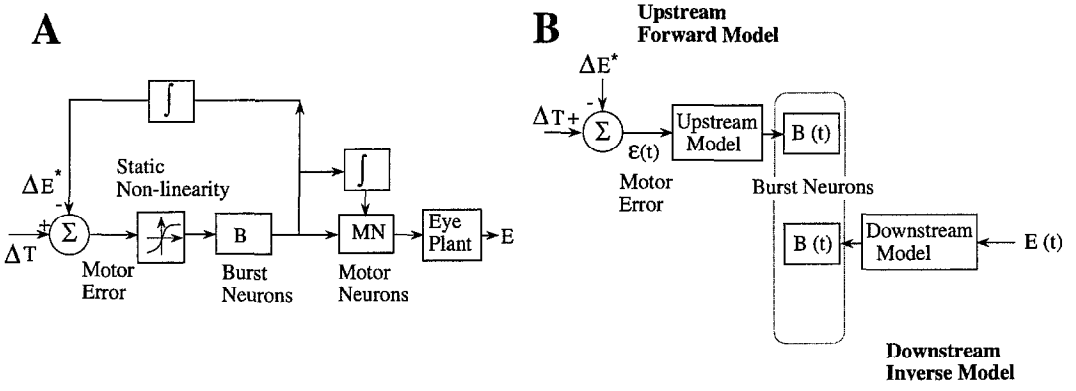

Figure 1. A) The classic local feedback model for saccade generation. This is the version proposed by Jurgens et al. (1981) as a modification to Robinson's (1964) early model. ΔE^* is the efference signal giving the angular rotation of the eye that has occurred since the onset of the saccade and is obtained by integrating the burst neuron output; this assumes that $B \propto \dot{E}$. ΔT is the desired angular rotation of the eye. E is the actual eye movement that is generated as a result of the motoneuron signal passing through the plant dynamics of the eye. B) Upstream forward and downstream inverse black-box models of the burster firing rate. $\varepsilon(t) = \Delta T - \Delta E^*$, the motor error signal that arises from A. This study focused exclusively on the downstream inverse model. The model is termed an inverse model because the algorithms we used required the system noise to appear at the output of the system. Consequently an inverse model was formulated to describe the downstream model studied in our analysis; that is, the more noisy burst neuron firing rate ($B(t)$) was estimated based on dynamic models in which eye movement ($E(t)$) was the input.

approximately described by $B(t) = b\dot{E}(t - t_d)$, where $B(t)$ is the burst neuron firing rate (Van Gisbergen et al., 1981).

In reality, it is necessary to use more elaborate models in order to describe the oculomotor plant (Robinson, 1964). A description of the motoneuron discharge that incorporates an eye acceleration ($\ddot{E}$) as well as an eye velocity term has been proposed (Keller, 1973; Van Gisbergen et al., 1981). These investigators further proposed that a better description of burst neuron firing rate can be obtained with

$$B(t) = f(\dot{E}(t - t_d)) + m\ddot{E}(t - t_d), \qquad (2)$$

where $f(\dot{E})$ is a nonlinear function of eye velocity and m is a constant.

Most recent models of motoneuron discharge patterns contain a pole term that appears as the derivative of the firing rate and permits the slow decline or "relaxation" of motoneuron activity after the eye position has reached steady state (Goldstein and Robinson, 1984; Optican and Miles, 1985; Fuchs et al., 1988). Such a term was present in the eye plant model originally proposed by Robinson (1964):

$$\begin{aligned} \mathrm{MN}(t) = r &+ b_0 E(t - t_d) + b_1 \dot{E}(t - t_d) \\ &+ b_2 \ddot{E}(t - t_d) - c\dot{B}(t) \end{aligned} \qquad (3)$$

and by extension

$$\begin{aligned} B(t) = r &+ b_0 E(t - t_d) + b_1 \dot{E}(t - t_d) \\ &+ b_2 \ddot{E}(t - t_d) - c\dot{B}(t), \end{aligned} \qquad (4)$$

where r, b_0, b_1, b_2, and c are constants and are not necessarily the same in Eqs. (3) and (4).

Equations (2) and (4) suggest a more general model for the firing rate of burst neurons based on eye dynamics in which there is a constant bias term, nonlinearities, and a pole in the system, for example,

$$\begin{aligned} B(t) = r &+ b_0 E(t - t_d) + b_1 \dot{E}(t - t_d) \\ &+ d_1 \dot{E}^2(t - t_d) + d_2 \dot{E}^3(t - t_d) \\ &+ b_2 \ddot{E}(t - t_d) - c\dot{B}(t), \end{aligned} \qquad (5)$$

where d_1 and d_2 are constants in the added terms that approximate the nonlinearity in Eq. (2). In this article we show how system identification methods can help us choose the important terms in Eq. (5). In this study, we have restricted our analysis to variations of Eq. (5) where either no pole term is included or where a pole term is considered but there are no nonlinear terms. However it is theoretically possible to extend the methods presented here to the general form of Eq. (5), in which the nonlinear terms are additive, since the derivation of the gradient is fairly straightforward (Sales and Billings, 1990; Johansen and Foss, 1993). Furthermore, it is also possible to extend these methods to nonlinear models in which the terms are not additive (as long as the gradient can be formulated); however, such models may not converge.

In each of the models described above, a delay (t_d) is included. This delay reflects in part the time required for the burst neuron activity to activate the motoneurons (axon conductance time and a synaptic delay) as well as the time required for activity in the motoneurons to drive the extraocular muscles (axon conductance time, synaptic delay, and muscle fiber activation times). Previous investigators have determined the lead time of burst neurons using one of two methods: (1) determining the onset of the first spike relative to the onset of the eye movement or (2) calculating the time at which the burst frequency exceeds a specific threshold value (see the review in Hepp et al., 1989). These methods share a common feature; only the beginning of the saccade-related burst is used to determine the lead time between the neuronal discharge and saccadic eye movement. There are a number of limitations inherent in using such a method to determine the latency to a step input: (1) the presence of noise in the firing discharge causes uncertainty in the time at which the discharge crosses a threshold (Fig. 2, panel 2); (2) the initial spikes may not drive the movement because it may require a number of spikes to depolarize the downstream neuron; and (3) as illustrated (Fig. 2) for a first-order system (Eq. (1), where $r = 0$ and the time constant, $\frac{b}{k} = 240$ ms), the lead time determined as the time the response crosses a threshold (bottom panel) is dependent on the input to system (top panel); a larger input results in a reduction in the apparent lead time, while in reality, the lead time for both inputs is the same. In our study, a neuron's "dynamic" lead time was determined by modeling dynamics between the system's input and output using all of the data in a saccade, not just the initial portion. This method produces the same estimate of latency, regardless of the amplitude of the input signal if the assumed model is appropriate. To evaluate lead-time we shifted the unit discharge in time (t_d) until an optimal model fit was obtained for a simple dynamic model which included

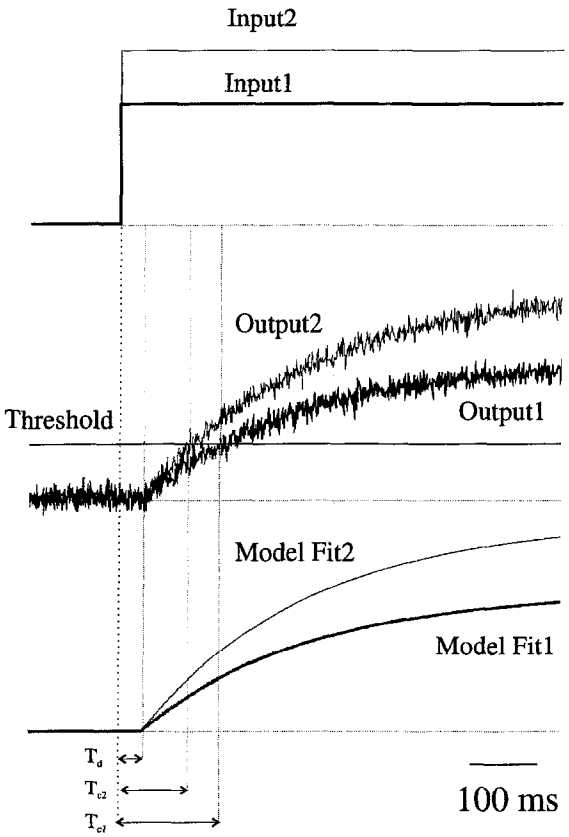

Figure 2. An example system demonstrating the limitations inherent in using a threshold in order to determine latency. The lead-time determined by the threshold method (second panel) is dependent on the noise as well as the amplitude of the input to system (top panel). In this example, a larger input will result in a reduction in the measured lead time (compare t_{c1} and t_{c2}). In contrast, if the lead time is determined by modeling the dynamics between the system's input and output ($\mathrm{MN}(t) = kE(t - t_d) + b\dot{E}(t - t_d)$) the estimate of latency (t_d) remains constant regardless of the amplitude of the input signal (bottom panel).

an eye velocity and bias term (discussed in more detail in a later section).

2. Methods

We employ system identification methods in order to objectively determine how well different formulations of Eq. (5) predict the discharge pattern of burst neurons in the cat and monkey. The methods fit burst neuron firing rate across many saccades simultaneously and automatically. In addition, we demonstrate that these techniques can be used both to provide an objective estimate of a neuron's dynamic latency and to test whether a neuron's initial firing rate (expressed as an initial condition) is linked to one of the quantities describing the saccade trajectories.

Equations (4) and (5) are inverse models since eye velocity is, in reality, the output of the system, and not the input as used here (see Fig. 1B). The reason for having burst neuron firing rate as the output is that the estimation algorithms we employed require that the noise be in the output (see below). The method used by Van Gisbergen et al. (1981) for fitting Eq. (2) requires interaction to remove the acceleration term by trial and error. We propose a simpler nonlinear regression algorithm for fitting Eq. (2). Regarding the more complex method that can also fit poles (or dependencies on the derivative of the firing rate) in models such as the ones in Eqs. (4) and (5), we utilized two versions of the more complex algorithm: one that uses the actual initial firing rate in the burst to estimate the initial conditions (B_0 in Eq. (7) below) and another that uses all of the saccades and fits the initial conditions as extra parameters.

2.1. *Dynamic Models for Firing Rate*

This section describes the methods used to estimate the parameters in the simple specific model described below by Eq. (6). A similar method was developed by Rey and Galiana (1993) for the analysis of the slow phase response of the vestibulo-ocular reflex (VOR). As in their method, we employ a least squares technique for the analysis, but our method differs from this. In their analysis, the VOR was characterized as a continuous response with transient deviations, whereas in our analysis of saccades the response is reinitialized for each saccade. In order to transform the continuous-time model in Eq. (6) into a discrete-time representation, a *backward-difference approximation* was employed. This procedure (also called the *Euler approximation*) is commonly used to produce digital simulations of analog systems. In the transformation, the derivative of a continuous-time function is approximated by the difference between two consecutive samples (moving backwards in time) of the signal to be differentiated (the linear difference equation).

In this section we (1) begin with a specific model (Eq. (6) below) expressed as a continuous-time equation, (2) formulate the z-domain representation of the model from the Laplace Domain representation, (3) formulate the linear difference equation from the z-domain representation in order to represent our model

as a discrete time series, and finally (4) express the linear difference equation in terms of the shift operator q^{-1} required by the System Indentification Toolbox of Mathworks Inc. (1987). The general formulation for this method is presented in the Appendix.

Consider the example of the continuous-time equation:

$$B(t) = r + b_0 E(t - t_d) + b_1 \dot{E}(t - t_d) - c\dot{B}(t). \quad (6)$$

This equation is represented in the Laplace Domain as

$$\mathbf{B}(s) = e^{-st_d} \frac{b_0 + b_1 s}{1 + cs} \mathbf{E}(s) + \frac{cB_0}{1 + cs} + \frac{r}{s}. \quad (7)$$

The formulation of $\mathbf{B}(s)$ in Eq. (7) emphasizes that the introduction of a $\dot{B}(t)$ term in Eq. (6) requires including (or estimating) initial conditions. By replacing $s = \frac{(1-z^{-1})}{T}$, where T is the sampling interval, and noting that the z transform representation of the Laplace transform e^{-st_d} is z^{-n_d}, Eq. (7) can be represented in terms of the corresponding z *transform*:

$$\beta(z) = z^{-n_d} \frac{b_0 T + b_1 - b_1 z^{-1}}{T + c - cz^{-1}} \xi(z) + \frac{cB_0 T}{T + c - cz^{-1}} + \frac{rT}{1 - z^{-1}}. \quad (8)$$

(A review of the basic properties of the z-transform can be found in Kuo, 1992.) By dividing the numerator and denominator of the first two terms by $(T + c)$, Eq. (8) becomes

$$\beta(z) = z^{-n_d} \frac{\frac{b_0 T + b_1}{(T+c)} - \frac{b_1 z^{-1}}{(T+c)}}{1 - \frac{cz^{-1}}{(T+c)}} \xi(z) + \frac{\frac{cB_0 T}{(T+c)}}{1 - \frac{cz^{-1}}{(T+c)}} + \frac{rT}{1 - z^{-1}}. \quad (9)$$

Then by defining

$$g_0 = (b_0 T + b_1)/(T + c) \quad (10a)$$

$$g_1 = -b_1/(T + c) \quad (10b)$$

$$f_1 = c/(T + c), \quad (10c)$$

Equation (9) can be rewritten as

$$\beta(z) = z^{-n_d} \frac{g_0 + g_1 z^{-1}}{1 - f_1 z^{-1}} \xi(z) + \frac{f_1 B_0 T}{1 - f_1 z^{-1}} + \frac{rT}{1 - z^{-1}}. \quad (11)$$

By rearranging terms Eq. (11) may, in turn, be expressed as

$$\beta(z) = z^{-n_d}(g_0 + g_1 z^{-1})\xi(z) + f_1 z^{-1}\beta(z) + f_1 B_0 T + \frac{rT(1 - f_1 z^{-1})}{1 - z^{-1}}. \quad (12)$$

Finally by taking the inverse z transform of Eq. (12) we obtain the linear difference equation:

$$\beta(n) = g_0 E(n - n_d) + g_1 E(n - n_d - 1) + f_1 B(n - 1) + f_1 B_0 TI(n + 1) + r(1 - f_1), \quad (13)$$

where in order to determine the inverse z transform of Eq. (12), the following basic properties of the z transform are utilized:

$$Z(x(n - n_d)) \Leftrightarrow z^{-n_d} X(z)$$

$$Z[r] \Leftrightarrow \frac{rTz}{z - 1}$$

$$rTf_1 z^{-1} = rTf_1, \quad \text{because } rTf_1 \text{ is a constant.}$$

In addition, note that the inverse z transform of a constant value is a delta function. In Eq. (13), the delta function is represented by the signal $I(n + nf)$, which is a discrete impulse at time $n = -nf$ samples, that is,

$$I(n + nf) = \begin{cases} 0 & \text{for } n \neq -nf \\ 1 & \text{for } n = -nf \end{cases},$$

where the first estimated value of $B^k(n)$ in the kth saccade will be for the sample interval designated $n = 1$.

The estimation of parameters was carried out, using the commercially available System Identification Toolbox (SIT) of Mathworks Inc. (1987), in which the available OE and ARX estimation routines were modified in order to account for, or estimate, the firing rate at the beginning of saccades in models with and without pole terms, respectively. The Matlab SIT requires a model formulated in terms of a polynomial in ascending powers of the shift operator q^{-1} defined by the relation

$$q^{-j} E(n) = E(n - j). \quad (14)$$

Accordingly, the linear difference equation in Eq. (13) can be expressed as

$$B(n) = q^{-n_d}(g_0 + g_1 q^{-1})E(n) + f_1 q^{-1} B(n) + f_1 B_0 T * I(n+1) + r(1 - f_1), \quad (15)$$

which can be further simplified to obtain

$$B(n) = q^{-n_d}\frac{(g_0 + g_1 q^{-1})}{(1 - f_1 q^{-1})}E(n) + \frac{f_1 B_0 T * I(n+1)}{(1 - f_1 q^{-1})} + r, \quad (16)$$

where the second term on the right emphasizes again that the introduction of a $\dot{B}(t)$ term in the time domain representation Eq. (6) requires including (or estimating) the initial conditions (B_0).

Equation (16) states that the burst frequency can be calculated exactly once the eye movement trajectory, and the initial conditions are known. However, this is unrealistic because there are other signals beyond our control that affect the system. Together, these can be called noise ($\gamma(n)$), and accordingly, $B(n)$ can be represented by a model of the form

$$B(n) = q^{-n_d}\frac{(g_0 - g_1 q^{-1})}{(1 - f_1 q^{-1})}E(n) + \frac{f_1 B_0 T * I(n+1)}{(1 - f_1 q^{-1})} + r + \gamma(n), \quad (17)$$

where $\gamma(n)$ is a noise term (not necessarily white).

The above model structure is called an output error (OE) formulation, which is one of a number of specific variants of the basic dynamic regression model structure, which is based on autoregression with exogenous inputs (ARX processes). The rationale for choosing OE models in the analysis of IBN discharges is addressed in the Discussion and Appendix.

Equation (17) describes a model of the discharge of a burst neuron during a single saccade (there is only one initial condition, B_0). In order to account for the effect of the firing rate at the beginning of *each* saccade, Eq. (17) is rewritten as

$$\beta^k(n) = q^{-n_d}\frac{(g_0 - g_1 q^{-1})}{(1 - f_1 q^{-1})}E^k(n) + \frac{f_1 B_0^k T * I(n+1)}{(1 - f_1 q^{-1})} + r^k + \gamma(n), \quad (18)$$

where: B_0^k is the initial state of firing rate occurring at the beginning of the kth saccade.

Note, that $g(q)$ and $f(q)$ do not have superscripts, since they are assumed to be shared by all saccades; whereas r^k the term allows the resting rate to be estimated separately for each saccade. The delay n_d was not solved for explicitly in all the models we tested. Instead, we first determined an optimal delay (n_d) by adjusting the value of n_d until the best fit of the burst neuron firing rate was obtained using an accurate model (see Section 3). This procedure enabled us to determine n_d more clearly and will be discussed in the subsequent section relating to Fig. 5. We used this particular value of delay to investigate the goodness of fit of other models; the eye movement data set was appropriately shifted in time by the estimated n_d. Equation (18) can be expressed as

$$B^k(n) = \frac{g(q)}{f(q)}E^k(n) + \frac{p^k(q)}{f(q)}I(n+nf) + r^k + \gamma(n), \quad (19)$$

where

$$g(q) = g_0 + g q^{-1}$$
$$f(q) = 1 + f_1 q^{-1},$$

and $p^k(q)$ is a representation of the unknown initial state of saccade k, which is proportional to (B_0^k), due to new set-points introduced before the kth saccade. The term $(p^k(q)/f(q))I(n+nf)$ therefore represents the transient component of the system—that is, the influence of the initial states of the system at the beginning of each saccade (B_0^k) on $B(n)$. Note, that the Laplace representation Eq. (7) required a similar term to represent the influence of initial conditions. In a model formulation in which there are no poles, this transient term is not needed. A schematic representation of Eq. (19) is illustrated in Fig. 9 for the single pole case.

In the specific model formulation given above, the number of poles (nf) = 1 and the number of zeros + 1 (ng) = 2. In an estimation in which ns was the total number of saccades, the total number of parameters (P) in Eq. (6) equals the number of parameters in $g(q)$, $f(q)$, plus the parameters for the initial states and a single bias (common to all saccades):

$$P = nf + ng + ns * nf + 1. \quad (20)$$

Since we used 40 saccades to estimate the parameters, $P = 1 + 2 + (40 * 1) + 1 = 44$ for this model. The

parameters in Eq. (19) are conveniently described as a column vector θ:

$$\hat{\theta} = \left[g_0, g_1, f_1, p_0^1, \ldots, p_0^{ns}, r\right]'. \tag{21}$$

The parameter estimates $\hat{\theta}$ ($\hat{}$ denotes the estimate of θ) were determined with Matlab using SIT. The particular model we have described above Eq. (19) has the OE structure with one pole. Parameters were estimated with a modified version of the OE function which takes into account initial conditions. Parameters were estimated using a one-step-ahead predictor, and the damped Gauss Newton algorithm for locating the minimal error (see details in the Appendix). For models in which there were no poles, we used an ARX function; the parameters in this model structure were estimated using the least squares method. The parameters θ describe the model in terms of Eq. (19). These parameters may, in turn, be transformed into the continuous time parameters b_0, b_1 and c using Eqs. (10a), (10b), and (10c).

The results of estimating parameters for models of various complexity are presented in the following section, beginning with a simple one-parameter equation in which burst frequency is proportional to eye velocity ($B(t) = b_1\dot{E}$). Increasingly complex models that incorporated combinations of the terms included in Eq. (5) were then tested. In order to determine which terms are most relevant for estimating the firing behavior of an IBN, we determined whether there was a decrease in the variance (VAR) of the fit, and a corresponding increase in variance-accounted-for (VAF) by the model when different terms were added to the simple model of the burst neuron's firing rate. The VAF was defined as $[(1-(\mathrm{VAR}/std))*100]$, where std is the standard deviation of the data set about a mean. The VAF in linear models is equivalent to the square of the correlation coefficient (R^2). Therefore, a model with a VAF of 64% actually provides as good a fit to the data as a linear regression analysis that yields a correlation coefficient of 0.80.

2.2. *Cost Function*

As reviewed by Caines (1988), model complexity should be considered a part of the criterion for an adequate fit. Otherwise, as the number of parameters in a system is increased, the predictor is likely to fit the output profile better (given that the input is sufficiently rich). Put another way, if more parameters are included in a model, it is natural to expect a decrease in fit error. Without penalizing for complexity one may choose a very high-order model even for the simplest of systems. By incorporating a criterion that restricts model complexity one can impose a tradeoff between complexity and error of the fit. There are several formulations for this tradeoff (see Caines, 1988 for a review). We present here one of them called the Bayesian Information Criterion (BIC) (Schwarz, 1978).

The BIC takes into account the automatic decrease in fit error that follows the addition of parameters to a model. In large samples, it produces a ranking akin to the posterior odds ratio, the ratio of probabilities of two models being correct given the available data (see Schwarz, 1978, and Zellner, 1984, for a discussion of the implications and applications of odds ratios). In effect, the BIC value indicates whether an increase in the complexity of the model is warranted considering the accompanying decrease in the error of the fit, that is, a decrease in the BIC value suggests that the increase in model complexity is warranted. We chose to use the BIC in this study, rather than the AIC (Akaike Criteria, another widely used cost function), since the AIC tends to be biased toward more complex models (Caines, 1988).

We have used minimum prediction error methods based on a least squares criterion. Least squares methods assume that the noise has a Gaussian distribution. In our case, the source of noise is hardly tractable, and a Gaussian assumption is made for the sake of simplicity. The choice of least squares is also a practical one since there are a number of very fast least squares algorithms in the literature. Define Ξ as the cost function (least squares) to be minimized:

$$\Xi(\hat{\theta}) = \sum_{n=1}^{N} \nu_n^2(n, \hat{\theta}),$$

where ν represents the error of the model fit at sample n. The BIC cost function is then defined as

$$\mathrm{BIC}(\hat{\theta}) = \log\left(\frac{1}{N}\Xi(\hat{\theta})\right) + \frac{P}{2}\frac{\log N}{N}. \tag{22}$$

This test penalizes the use of a large number of parameters (P) relative to the number of data points in the input (N).

2.3. Experimental Methods

To illustrate the use of the optimization algorithms outlined above, we analyzed as, stated in the Introduction, the firing behavior of IBNs. The surgical preparation of the animals and methods used for obtaining the extracellular recordings from brainstem neurons were similar to those previously described (cat: Pare and Guitton, 1990; monkey: Cullen and McCrea, 1993). One cat and one monkey were prepared for chronic extracellular recording. The IBNs described in this study were identified on the basis of their characteristic "burst" discharge during horizontal saccadic eye movements in the ipsilateral direction and their location in the "IBN area" caudal and ventral to the abducen's nucleus (Fig. 3, and see descriptions in Hikosaka and Kawakami, 1977; Kaneko and Fuchs, 1981; Yoshida et al., 1982; Scudder, 1988). These neurons were also characterized as IBNs based on their responses during quick phases of vestibular nystagmus evoked during rotation of the vestibular turntable and by their lack of response during slow phases of nystagmus and smooth pursuit eye movements.

The cat and monkey were trained to orient to a food target that appeared unexpectedly on either side of an opaque screen (see Guitton et al., 1984, for details). In addition, the monkey was trained to orient for a juice reward to a target light that was projected on a cylindrical screen (Cullen and McCrea, 1993). The target was stepped horizontally between positions 5, 10, 20, and 35 degrees relative to the straight ahead position. Burst neuron activity was recorded during saccades made with the animal's head held fixed. Eye movements were recorded using the magnetic search coil technique. Eye position signals were stored with the recorded unit activity on DAT tape (5 kHz sampling frequency). The recorded eye position signals were low-pass filtered (250 Hz, 8 pole Bessel) and digitized at 1000 Hz. Fourier analysis of human and monkey ocular saccades has revealed little power above 50 Hz (Zuber et al., 1968; Van Opstal et al., 1985; Harris et al., 1990). Fourier analysis of cat ocular saccades, in this study, revealed little power above 30 Hz (Fig. 4A, top panel). This is consistent with our observation that cat saccades tend to be slower than humans and monkey saccades of the same amplitude. Traces were digitally filtered at 60 Hz (cat) and 125 Hz (monkey). A low-pass finite-response digital filter (order = 50) was applied in both forward and backward directions so as to ensure zero-phase filtering (Matlab, Signal Processing toolbox). Saccades in which the vertical displacement component was more than one-third of the entire saccade amplitude were not included in this analysis. We analyzed only the horizontal component of each saccade. The onset and offset of a saccade were defined using a ±20 deg/s eye velocity criterion. In the analysis we shifted the burst in time relative to the saccade by the estimated latency (see below), and then only that portion of the burst that was coextensive with the saccade duration was used to fit a model.

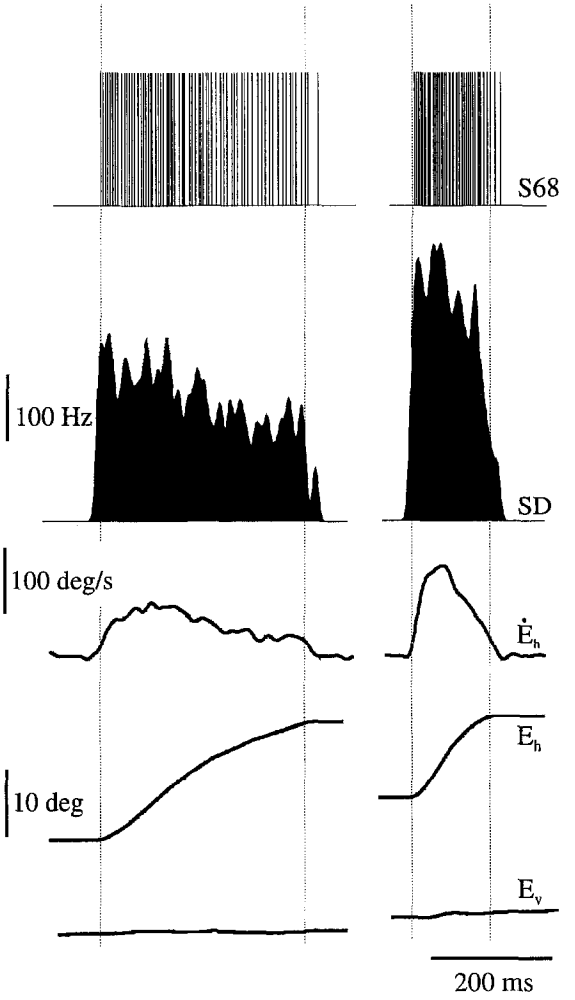

Figure 3. Example of the firing rate of a cat IBN (unit S68) during two horizontal saccadic eye movements in the head-fixed condition. Spike density (SD) (second row) was obtained by replacing each spike (top row) by a Gaussian of 5 ms width. The corresponding horizontal eye velocity ($\dot{E}_h$), and horizontal (E_h) and vertical eye position (E_v) traces are shown in the bottom three rows, respectively. Dashed vertical lines indicate the onset and offset of the saccade using a 20 deg/s eye velocity criterion.

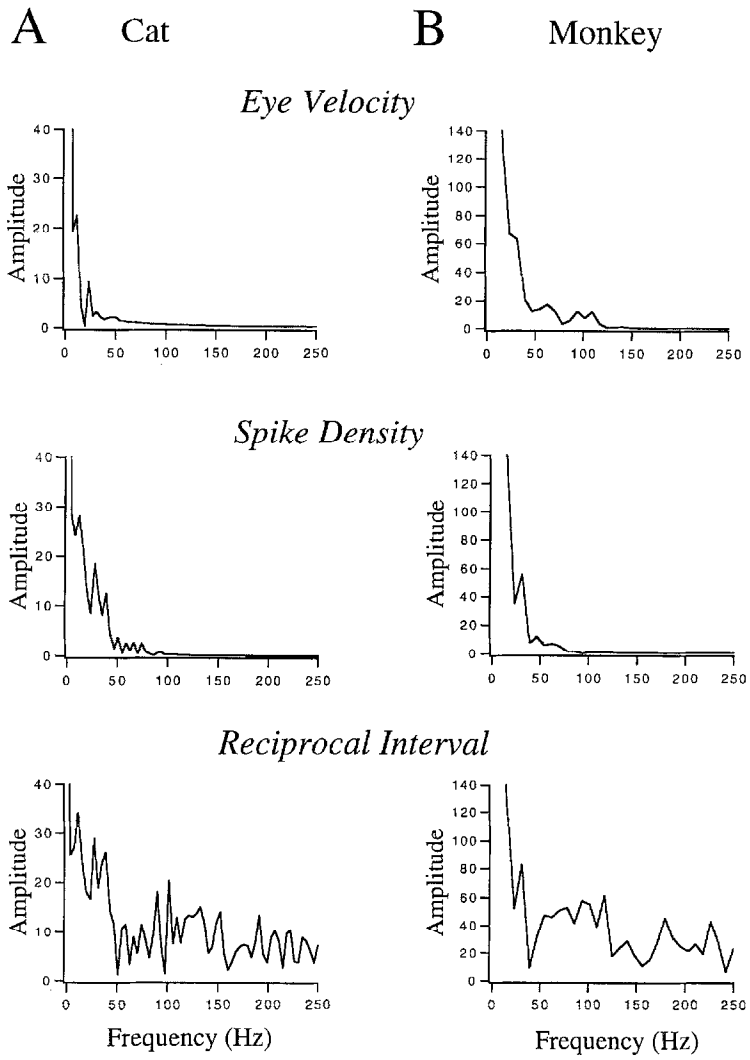

Figure 4. The frequency composition (determined using the fast Fourier transforms algorithm) of saccadic eye velocity (top row) and two measures of neuron discharge: (1) the spike density function (second row) which was obtained by convolving the spike train function with a Gaussian pulse, and (2) the reciprocal of the interspike interval (third row). Plots are shown for data from cat (A) and monkey (B). Note that the duration of the illustrated 20 degree saccade was longer for the cat than for the monkey by a factor of ≈ 2. For this reason the amplitude spectra of the cat data contains twice as many points as that of the monkey. The choice of a 5 ms width for the Gaussian permitted us to effectively low-pass filter the neural discharge at a frequency comparable to that used for filtering the eye movement signal (compare rows 2 and 1, respectively). Consequently, there was no significant signal above about 100 Hz for either the eye velocity or spike density representation of the firing rate. In contrast, the reciprocal interval method (third row) resulted in a representation of firing rate that contained significant signal at much higher frequencies.

The event times of the neuronal action potentials were logged, and corresponding spike trains were calculated (see Cullen and McCrea, 1993, for details). We employed a spike density function (Parzen analysis) to represent the discharge of the burst neurons (Fig. 3). This function was obtained by convolving the spike train function with a Gaussian pulse. We chose this method, rather than the reciprocal of the interspike interval, to calculate the instantaneous firing frequency of the neuron, since it has the advantage of being linear, whereas the reciprocal interval method is nonlinear and sensitive to noise especially at high frequencies (Sanderson and Kobler, 1976; Richmond et al., 1987). The sensitivity of the reciprocal interval method to noise at high frequencies is apparent in the example illustrated in Fig. 4 (lower panels). In addition, by using a Gaussian of appropriate width (standard deviation of 5 ms), it was possible to low-pass filter the

neural discharge such that it and the eye movement signals contained energy over a similar frequency range. This is demonstrated in Fig. 4, where the frequency composition of the eye velocity (top panels) is comparable to that of the spike density (middle panels), whereas the reciprocal interval representation of firing discharge (bottom panels) contains significant signal power at higher frequencies. We found that (1) decreasing the width of the Gaussian used in the Parzen analysis by 50% and/or (2) reducing by 30% the cut-off of the low-pass filter used on our eye movement records had little effect on the results presented below (both the estimated latencies and parameters were not markedly changed).

3. Results of Applying the Parameter Estimation Methods

Using the methods detailed above in Section 2, we first computed latency by adjusting the value of the delay t_d to the nearest millisecond until we obtained the best fit to the burst neuron firing rate using the simple equation

$$B(t) = r + b_1\dot{E}(t - t_d) \tag{23}$$

and the more complex equation:

$$B(t) = r + b_0E(t - t_d) + b_1\dot{E}(t - t_d) - c\dot{B}(t) \tag{6}$$

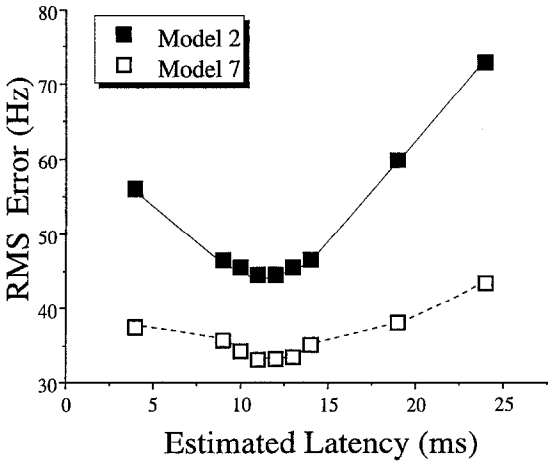

Figure 5. Example of the resulting errors from fitting a cat IBN's firing rate using a simple downstream model (2, closed symbols)—$B(t) = r + b_1\dot{E}(t - t_d)$—and a more complex downstream model (7, open symbols)—$B(t) = r + b_1\dot{E}(t - t_d) + b_2\ddot{E}(t - t_d) + c\dot{B}$—using different latencies (t_d). The optimal dynamic latency was 12 ms for both models; however, the simple model was considerably more sensitive to latency than the complex model.

These two models correspond to rows 2 and 7 of Table 1. Figure 5 illustrates the RMS error of fit at latencies near the optimal for these two models. The value of t_d that led to the best fit (minimum RMS error) provided our estimate of the dynamic latency. Figure 5 also illustrates that using a more complex model with many parameters makes it more difficult to optimize

Table 1. RMS, VAF, and BIC values for the downstream models tested.

			S68			HO721		
Model	Global fits to 40 horizontal saccades	Params	RMS[a]	VAF[b]	BIC[c]	RMS[a]	VAF[b]	BIC[c]
1	$B(t) = b_1\dot{E}(t - t_d)$	1	75.7	25	8.65	181.1	−10	10.40
2	$B(t) = r + b_1\dot{E}(t - t_d)$	2	44.5	56	7.59	101.7	38	9.25
3	$B(t) = r + b_1\dot{E}(t - t_d) + d_1\dot{E}^2(t - t_d) + d_2\dot{E}^3(t - t_d) + b_2\ddot{E}(t - t_d)$ (Van Gisbergen et al., 1981)	5	41.3	59	7.45	100.3	39	9.23
4	$B(t) = r + b_1\dot{E}(t - t_d) + b_2\ddot{E}(t - t_d)$ (Approximation to Van Gisbergen et al., 1981)	3	41.8	59	7.47	101.4	39	9.24
5	$B(t) = r + b_0E(t - t_d) + b_1\dot{E}(t - t_d)$	3	46.7	54	7.69	97.1	41	9.16
6	$B(t) = r + b_1\dot{E}(t - t_d) + b_2\ddot{E}(t - t_d) + c\dot{B}(t)$ (Initial conditions taken from data)	4	41.0	59	7.43	96.8	41	9.15
7	$B(t) = r + b_1\dot{E}(t - t_d) + b_2\ddot{E}(t - t_d) + c\dot{B}(t)$ (Initial conditions estimated as parameters)	4 (40 initial)	32.9	67	7.11	77.8	53	8.77
8	$B(t) = r + b_1\dot{E}(t - t_d) + b_2\ddot{E}(t - t_d)$ (Bias estimated as parameter)	2 (40 biases)	32.3	68	6.98	78.8	52	8.79

[a]Root mean square error.
[b]% variance accounted for.
[c]Bayesian information criterion.

the value of latency. This is due to two factors. First, estimating the latency increases the number of parameters from 2 to 3 in Eq. (23) and from 44 to 45 in Eq. (6). Hence, changing the value of one parameter in Eq. (6) has relatively little influence on the optimized result compared to changing one parameter in Eq. (23). Second, the values estimated for the initial conditions are themselves related to latency. Accordingly, in the results that follow, for each cell the delay (n_d) was set to that value which provided the best fit of firing rate using the simple model in Eq. (23) corresponding to row 2 of Table 1.

Table 1 illustrates the RMS errors and VAF and BIC values of different model fits for one cat IBN (S68) and one monkey IBN (H0721). Row 1 illustrates the performance of the simplest downstream model we tested that relates unit discharge to eye velocity using only a gain term. For the monkey neuron, the variance of the model's fit error was actually larger than the variance of the data (indicated by the negative sign preceding the VAF value). Comparison of these values with those obtained when a bias term (r) was added to the model (row 2), indicates that a bias term greatly improved the fit of the model for both neurons studied. Note that this model (VAF = 56% (cat) and 38% (monkey)) actually provided a fit to the data that was as good as that described by correlation coefficients of 0.75 and 0.62, respectively, in a linear regression analysis. In addition, the accompanying dramatic decrease in the BIC values for both neurons suggests that the addition of a bias term to the model is warranted. Examples of the improvement in the fit of IBN firing rate that occurred with the addition of a bias term are illustrated for the cat IBN in Fig. 6 (compare top two panels). Note the excellent fit to even local variations in firing rate.

In order to investigate the hypothesis of Van Gisbergen et al. (1981) that, in a downstream model, unit firing can be represented by the addition of a nonlinear function of eye velocity and an eye acceleration term, a model based on Eq. (2), which included a third-order nonlinearity and an eye acceleration term but no pole term, was tested (Table 1, row 3). For each neuron the addition of the higher-order eye velocity terms (d_1 and d_2) and acceleration term (b_2) decreased the error of the model, but the addition of these terms was far less effective in decreasing the VAF than the addition of the bias term had been originally. In addition, a more simple approximation to the model of Van Gisbergen et al. was tested (row 4), in which the proposed nonlinearity in velocity was expressed, as in row 2, by $r + b_1\dot{E}(t - t_d)$. This formulation of the nonlinearity

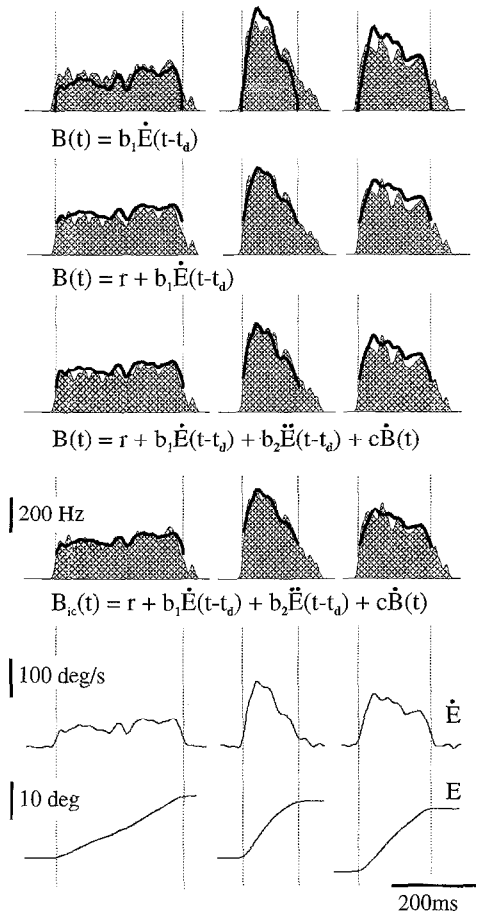

Figure 6. Examples of best fits of IBN firing rate during head-fixed saccades for an example cat neuron (S68). First and second panels: the addition of a bias term greatly improved the model fit based on eye velocity (compare top panel (no bias term) and second panel (bias and eye velocity terms)). See Tables 1 and 2 (rows 1 and 2). Third and fourth panels: examples of the improvement of the fit of cat IBN (S68) firing rate with the addition of acceleration and pole terms to an eye velocity based model. Third row: initial conditions $B_0(t)$ are taken from data (see Tables 1 and 2, row 6). Fourth row: ixnitial conditions are estimated as parameters (see Tables 1 and 2, row 7).

In the top four panels the shaded area shows actual firing frequency, and the solid line the estimated firing based on the equation given below each panel. The parameters are given in Table 2. The corresponding horizontal eye velocity ($\dot{E}$) and eye position (E) traces (bottom two rows) are illustrated for each of the three saccades, which were of about the same amplitude but had quite different trajectories.

provided as good a fit to the data as one that incorporated a higher-order nonlinerity (compare rows 3 and 4). The significance of eye position in determining the firing of IBNs was also investigated (row 5). For the monkey neuron this term was actually more relevant than the acceleration term (row 4) in estimating the unit discharge, while the reverse was the case for the

cat neuron. For both of the neurons, the addition of acceleration, higher-order velocity and position terms (in rows 3, 4, and 5) only slightly reduced the BIC values from those calculated for the model that included only velocity gain and bias terms (row 2).

A modification to the model in row 5 was also investigated (row 6), which in addition to bias, acceleration, and linear eye velocity terms allowed for the estimation of a pole in the system. The addition of this term provided only a slightly better model fit of the data when the initial conditions were taken from the data (compare VAF in rows 4 and 6). However, when the initial conditions were estimated as parameters, this model improved the fit considerably (compare VAF in rows 6 and 7). Example fits to firing rate when initial conditions were (1) taken from data and (2) estimated as parameters are shown in the third and fourth panels of Fig. 6, respectively. When the initial conditions were estimated as parameters, the fits to the data were as good as those described by correlation coefficients of 0.82 and 0.72 in a linear regression analysis, for the cat (VAF = 68%) and monkey (VAF = 52%) neuron, respectively. The improved fits, associated with this more complex model, can be observed by eye (compare third and fourth panels).

Because estimating the initial conditions as parameters added a large number of parameters to the estimation algorithms (equivalent to the number of saccades included in the analysis), it was important to check whether the corresponding BIC value also decreased. A comparison of the BIC values in rows 4 and 7 indicated that the large increase in model complexity was warranted. In the final downstream model that was investigated (row 8), the bias term was estimated separately for each saccade which was analyzed. This particular model formulation was of special interest for two reasons: (1) the method of estimation is simpler than for models which include a pole term and (2) a variable bias might have specific physiological implications. The errors based on this model are illustrated in row 8. The model fits were as good as those based on the model which included a pole term and for which initial conditions were fit as parameters (compare rows 7 and 8).

The values that were estimated for the parameters in each of the eight downstream models are shown in Table 2. It is not our intention here to interpret, in detail, the significance of particular and relative values of each parameter as well as the significance of different models. This is reserved for a subsequent paper in which we will present data on our complete population of burst neurons. For our demonstration sample of two neurons, the most relevant inputs (or terms) to predict IBN firing rate are eye velocity and the bias term. The sign of the estimated eye velocity term was positive in each model, indicating that the firing rate increased with increasing eye velocity in the neuron's "on" direction (ipsilateral) as would be expected from previous studies of IBNs. For the cat neuron (S68), the estimated bias terms were similar for all models, with the exception of the third-order nonlinear representation of the Van Gisbergen et al., model (row 3). In this latter model, the bias term was generally slightly lower, and eye velocity gain was correspondingly higher, as might be expected from a curvilinear fit. For the monkey neuron, the bias term was the lowest in the model of row 7, and again the velocity gain was higher. For both neurons, there was no indication that the bias term decreased with either increasing model complexity or increasing VAF.

Although, the addition of an acceleration term to the downsteam model slightly improved the fit for both neurons, its value was very low and of little consequence given the very small accompanying change in the BIC value. A surprising outcome of the analysis was that the sign of the estimated eye position term between cat and monkey varied (Table 2, row 5), but the influence of the position term was small compared to the bias term for both cat and monkey neurons.

One advantage of identification methods is that they permit a quantitative evaluation of initial conditions (row 7) and their relation to other movement characteristics. As an example Fig. 7 illustrates, for primate neuron (H0721), the strong correlation between the

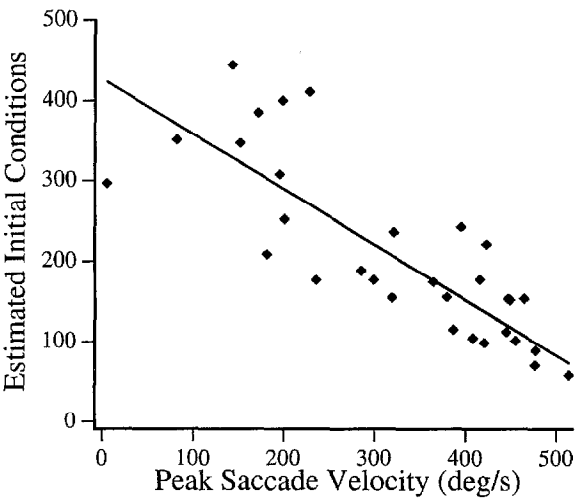

Figure 7. Linear regression analysis ($r = -0.82$) of the relationship between the estimated initial conditions (Fig. 6 fourth row) and peak velocity of saccades for primate neuron H0721.

Table 2. Parameter estimations for the models tested.

	Global fits to 40 horizontal saccades	Parameters		Parameter estimates and SDs S68	HO721
1	$B(t) = b_1 \dot{E}(t - t_d)$	1	$b_1 = \pm$	3.5/0.1	1.82/.01
2	$B(t) = r + b_1 \dot{E}(t - t_d)$	2	$r = \pm$	133.1/1.3	306.5/4.2
			$b_1 = \pm$	2.18/.01	.79/.02
3	$B(t) = r + b_1 \dot{E}(t - t_d) + d_1 \dot{E}^2(t - t_d)$	5	$r = \pm$	108.6/4.0	287.4/9.9
	$+ d_2 \dot{E}^3(t - t_d) + b_2 \ddot{E}(t - t_d)$		$b_1 = \pm$	2.8/0.1	0.9/0.2
	(Van Gisbergen et al., 1981)		$d_1 = \pm$	−.004/.001	.0008/.0008
			$d_2 = \pm$	.0000/.0000	.0000/.0000
			$b_2 = \pm$	.0063/.0002	−.0002/.0002
4	$B(t) = r + b_1 \dot{E}(t - t_d) + b_2 \ddot{E}(t - t_d)$	3	$r = \pm$	134.3/1.3	310.8/4.3
	(Van Gisbergen et al., 1981)		$b_1 = \pm$	2.2/0.1	.78/.02
			$b_2 = \pm$	.0064/.0002	−.0002/.0002
5	$B(t) = r + b_0 E(t - t_d) + b_1 \dot{E}(t - t_d)$	3	$r = \pm$	131.0/1.8	299.8/4.2
			$b_0 = \pm$	.62/.13	−.70/.09
			$b_1 = \pm$	2.2/0.2	.78/.02
6	$B(t) = r + b_1 \dot{E}(t - t_d) + b_2 \ddot{E}(t - t_d) - c\dot{B}(t)$	4	$r = \pm$	137.9/1.3	336.2/4.7
	(Initial conditions taken from data)		$b_1 = \pm$	2.1/0.2	.66/.07
			$b_2 = \pm$	.0143/.0005	.01/.10
			$c = \pm$	.003/.09	.0113/.0003
7	$B(t) = r + b_1 \dot{E}(t - t_d) + b_2 \ddot{E}(t - t_d) - c\dot{B}(t)$	4	$r = \pm$	138.1/4.3	104.0/40.3
	(Initial conditions estimated as parameters)	(40 initial)	$b_1 = \pm$	1.7/.2	1.3/0.1
			$b_2 = \pm$	.239/.002	.10/.10
			$c = \pm$	.13/.08	.099/.002
8	$B(t) = r + b_1 \dot{E}(t - t_d) + b_2 \ddot{E}(t - t_d)$	2	$b_1 = \pm$	1.9/.01	1.01/.02
	(Bias estimated as separate parameters)	(40 biases)	$b_2 = \pm$	.0065/.0002	−.0002/.0001

estimated initial conditions and the peak velocity ($r = -.82$) of the saccade. The generality and significance of this observation, as well as those relating to model structure, will be considered in a subsequent report on our entire population of cells.

4. Discussion

The aim of system identification is to build a mathematical model of a dynamical system that best describes the data obtained from that system. This article presents the first attempt to use system identification techniques to investigate neural signals in the brainstem burst generator that drives eye saccades.

The generalized model structure of a linear system is (Ljung, 1987, p. 77)

$$A(q)y(t) = \frac{B(q)}{F(q)}u(t) + \frac{C(q)}{D(q)}e(t),$$

where A, B, C, D, and F are polynomials in the shift operator q^{-1}; $u(t)$ is the sampled input, $y(t)$ the sampled output, and $e(t)$ the noise.

Parameter estimation in such complex systems suffer from convergence and consistency problems; most practical applications involve setting to unity, one or several of the polynomials. In all the parameter estimation algorithms used in this study, we assume that the system noise appears only on the observed system output Fig. 9 (output-error (OE) representation; see Ljung 1987, p. 75). This is equivalent to allowing for neural and/or instrumentation/measurement noise on burst cell activity. In OE systems, estimation algorithms are easily available and have been shown to converge to accurate parameter estimates for any type of nonzero noise. However, we have used an OE formulation not only because of its mathematical tractability but because it is also a plausible representation of the saccade burst generator. The burst generator (IBNs and

EBNs) is monosynaptically connected to motoneurons (MNs), which in turn drive the eye plant. In this system, the major "noise" sources come from (1) other neurons that project to MNs and discharge during saccades; this would include other burst neurons, cells in the vestibular-prepositus hypoglossi complex (Baker et al., 1981; Cheron et al., 1986a, 1986b; Cheron and Godaux, 1987; Escudero et al., 1992; Lopez-Barneo et al., 1982; Mettens et al., 1994), as well as modulators that effect alertness and behavioral set; (2) other motoneurons that are not driven by the particular burst neuron being analyzed; and (3) transmission noise in the IBN-MN and MN-muscle synapses. These noise sources can be assumed to act on burst neurons (i.e., the OE model) if the dynamics between the burst neuron and MNs are negligible, compared to those imposed by the eye plant. However, we know of no data to support such an assumption. We discuss this topic further in the last section.

In our estimation algorithm, we use the equivalent of a z transform to represent burst neuron discharge. Our data was sampled at 1 kHz, and if the parameters estimated for the pole terms had approached unity (their maximum value, see Eq. (10c)), then small differences in the estimation of these parameters would have corresponded to large differences in the estimated time constant of the transient. In such a case, the estimation algorithms could become ill conditioned (Rey, 1992). However, in our analysis the estimated pole terms did not approach 1, so this issue was not a concern. Nevertheless, it is possible that such a problem would be relevant in the potential analysis of oculomotor neurons, which are active during slow eye movements and fixation as well as during saccades, since it is likely that the relevant dynamics may differ for slow versus fast eye movements. Recently, it has been demonstrated that an ARX parameter estimation algorithm based on a "delta" representation for the discrete domain is more numerically stable than that based on the traditionally used z transform representation (Vijayan et al., 1991; Pintelon and Kollar, 1991). In the delta representation, added stability is obtained by accounting for the sampling interval used in the estimation. Consequently, the delta representation has the advantage that the estimated parameters change little with sampling rate. We suggest that a logical extension of the analysis techniques described above would be to estimate the parameters for a set of OE models, in which the firing behavior of neurons active during slow and fast eye movements is represented in terms of a delta transform.

4.1. Prior Analyses of Burst Neuron Discharge

Our approach has the major advantage of providing an objective evaluation (the BIC index) of whether it is warranted to use additional parameters in order to improve a goodness of fit. Most prior analyses of burst neuron activity have been based on a first-order model of the eye plant mechanics, combined with the hypothesis that activity in burst neurons creates the burst in motoneuron activity, which in turn generates saccades. In this context one would expect, as reviewed by Van Gisbergen et al. (1981), that $\dot{E}(t)$ is well predicted by $B(t)$. Accordingly, prior analyses of burst neuron discharge in relation to saccadic eye movements have largely focused on either the relationship between peak eye velocity and peak discharge frequency or on global characteristics of the discharge, such as the relationships between number of spikes and saccade amplitude and between burst duration and saccade duration.

These relationships do not consider the link on a moment to moment basis between the burst and velocity profiles. A further major difficulty is the calculation of latency, which in prior analyses has not been based on functional criteria. For the so-called short-lead burst neurons whose firing begins with an abrupt increase in frequency, the latency is usually taken as the time between the first spike in the burst discharge and the start of the movement. For burst neurons that begin with a low-frequency prelude, the so-called long-lead burst neurons (LLBNs) latency is defined arbitrarily as the point in time where the frequency changes from low to high (e.g., Scudder, 1988). Such definitions have limited functional significance as discussed with relation to Fig. 2. For example, output neurons of the cat's superior colliculus can begin discharging 25 ms or more before a movement, but once the movement is underway, an increase in spike frequency leads to an acceleration of the eye 10 ms later (Munoz et al., 1991). Electrical stimulation of the SC has the same properties: latency of movement to stimulation onset is longer than eye acceleration to a sudden increase in stimulus frequency when the evoked movement is underway (Munoz et al., 1991). The methods discussed in this article overcome these problems and define latency functionally in relation to the average effect of every spike in the burst on the movement trajectory.

One attempt to correlate movement trajectory with burst frequency profile was made by Van Gisbergen et al. (1981) using phase-plane trajectories. For the downstream model they plotted average values of $\dot{E}(t)$

versus $B(t)$ for saccades of a given size and direction. They found that $\dot{E}$ was predicted best, not by $B(t)$, but by $B(t) - \mu\ddot{E}(t)$ (where μ is a constant), indicating that both eye velocity and acceleration are determined by the burst discharge (see Eq. (2)).

There are a number of difficulties in the approach of Van Gisbergen et al. First, their calculation of a neuron's instantaneous discharge was based on the reciprocal of the interspike interval. Spike frequency calculated in this manner is nonlinear and increasingly sensitive to noise at high frequencies of discharge, whereas the spike density function rises linearly with increasing frequency (Sanderson and Kobler, 1976; Richmond et al., 1987). In the Van Gisbergen et al. analysis, eye position signals were low-pass filtered at 180 Hz; however, the representation of the burst neuron firing rate contained much higher frequency components. It is possible that their analysis introduced unwarranted high-frequency signals between input and output, which enhanced their estimate of the effect of eye acceleration. We have avoided this difficulty by using the linear Parzen analysis with a Gaussian pulse width, which effectively filtered the neural activity at a frequency similar to that used for filtering the eye movement signals. Second, their graphical approach is cumbersome, and although it can be refined using computer-aided numerical approaches, the method does not lend itself to verifying more complex models such as the ones with pole terms as in Eq. (5). Third, in order to correct for latency in their investigations, they determined the time between the onset of the burst (defined as when the discharge rate exceeded 100 spikes per second) and the saccade. As discussed above, this method of determining latency is different from the dynamic estimate of latency that we have employed, and it is possible that their method introduced the equivalent of a phase-lead in unit discharge relative to eye velocity leading to an overestimate of the eye acceleration coefficient. Such an effect is illustrated in Fig. 8. The top panel shows the fit and value of the acceleration coefficient (b_2) for the optimal latency (t_d). The subsequent two lower panels show the effect on the estimate of b_2 of decreasing and increasing t_d by 5 ms, respectively.

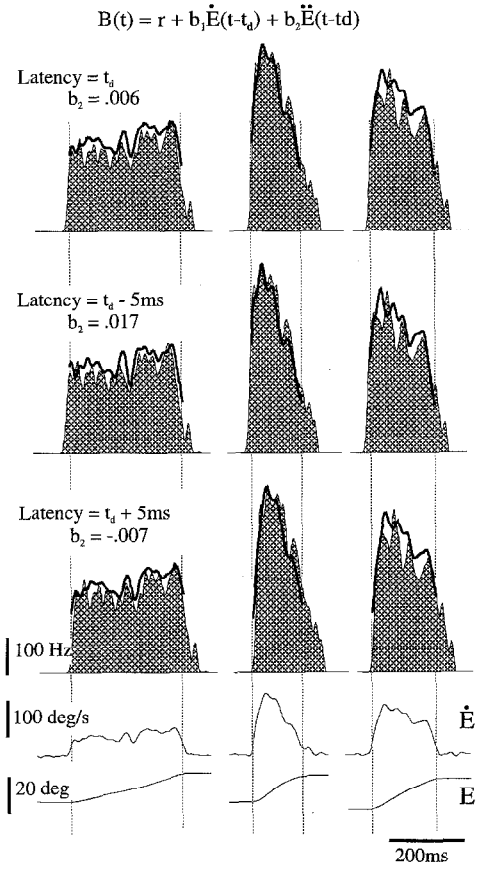

Figure 8. The firing rate of a cat IBN (S68) is fit with a model containing a bias term and eye velocity and acceleration term in order to approximate the model proposed by Van Gisbergen et al. (1981). When the optimal dynamic latency (t_d) was used the estimated eye acceleration coefficient was quite small ($b_2 = .006$, top row); whereas, using a smaller dynamic latency ($t_d - 5$ ms) resulted in a significantly larger estimated value for the eye acceleration coefficent ($b_2 = .017$, second row). When the dynamic latency was chosen to be larger than t_d, the estimated value for the eye acceleration coefficent reversed in sign ($b_2 = -.007$, third row). Results shown are from the same three saccades that are illustrated in Fig. 6. Note that the VAF for the entire data set of 40 saccades to which each model was fit were 41.8, 47.2, and 45.3 for rows 1 to 3, respectively. In the top three rows, the shaded area shows actual firing frequency, and the solid line the estimated firing. The corresponding horizontal eye velocity ($\dot{E}$) and position (E) traces for each of the three saccades are shown in the bottom two rows.

4.2. *Significance and Usefulness of the Models*

The algorithm presented here, allows one to objectively investigate (1) a burst neuron's dynamic latency, (2) how well a given model predicts a neuron's discharge pattern, (3) whether increasing the complexity of a model is justifiable, as well as (4) the relationship between initial conditions and quantities describing the saccades' trajectories. In our estimation of dynamic latency we specifically investigated the effect of varying the dynamic latency on the ability of two models, a simple model (Model 2) and more complex model

(Model 7) to predict neural discharges. While the optimal value estimated for the dynamic latency was consistent between the two models, the simple model was more "latency tuned" (Fig. 5). It is important to note that in our analysis we always assumed a fixed delay for a given neuron. However, previous studies have suggested that latency could vary on a saccade by saccade basis for a single cell; for example, in the case of burst neurons it has been shown that latencies vary with saccade direction (Kaneko and Fuchs, 1981). Accordingly, one future application of these techniques might be to probe whether the dynamic latency is in fact a fixed value for a given neuron or whether it varies in a systematic manner from saccade to saccade or even throughout the course of a single saccade.

In the present study we have also demonstrated that the addition of a bias term to an eye velocity-based model greatly improved our ability to predict our neuron's discharges. In contrast, we found that increases in model complexity—which included adding eye acceleration, position and nonlinear velocity terms—provided only a minor improvement in our ability to fit burst neuron firing profiles. However when models included a pole term as well as eye velocity, acceleration, and bias terms, a marked improvement in model fit was noted. This class of model was particularly adept at describing neuron discharges when the initial conditions were estimated as parameters. When initial conditions were estimated as parameters (Model 7), we found that a strong relationship existed between the estimated initial conditions and peak saccade velocity for unit H0721 (illustrated above in Fig. 7). However, a similar relationship was not present when initial conditions were taken directly from the data (Model 6). It is interesting to note that in Model 7, the values estimated for the parameter c was $\approx$100 ms for both neurons. This parameter is the time constant of the decay of the initial conditions, and it is long relative to the duration of a saccade. Hence, the initial conditions effectively became a bias that varied for each saccade, and it is not surprising that the VAFs obtained using Models 7 and 8 (the multiple bias fit model) were nearly equivalent.

In the brainstem oculomotor circuitry, there are many discrete and interlinked nuclei or zones, each of which contains output neurons having more or less the same discharge characteristics. This organization has facilitated the generation of models in which a neural circuit is built using single representative cells, each of which is a lumped representation of the properties of the output neurons in its class (for the saccadic system see for example, Robinson, 1975; Van Gisbergen et al., 1981; Scudder, 1988; Galiana and Guitton, 1992). A simple version of such a model has been shown in Fig. 1A, where burst neurons and motor neurons are represented by single black boxes. In this model, burst neuron firing rate is related simultaneously "upstream" to a motor error signal and "downstream" to the dynamics of the saccade. While in this study we have concentrated on estimating IBN activity based on downstream signals, the techniques presented could be similarly employed in order to develop a model of burst neuron firing rate based on an upstream error signal. We will show this in a subsequent paper on our population of cells.

Apart from burst neurons, another input onto motor neurons in Fig. 1A is the so-called neural integrator, which is thought to be a neural network involving neurons in prepositus hypoglossi (PH) and vestibular nuclei (VN) (Baker et al., 1981; Cheron et al., 1986a, 1986b; Cheron and Godaux, 1987; Escudero et al., 1992; Lopez-Barneo et al., 1982; Mettens et al., 1994). This black box is hypothesized to receive an eye velocity signal—a first approximation to burst neuron discharge—and to output an eye position signal that follows the burst on motoneurons. In reality, the output of the neural integrator contains signals that also contribute to motoneuron discharges during saccades; and, as mentioned earlier, it is likely that there are additional inputs to motoneurons, from other saccade-related discharges in the VN-PH complex (Cullen et al., 1993; Scudder and Fuchs, 1992; McFarland and Fuchs, 1992) and superior colliculus output cells (Grantyn and Berthoz, 1985). Due to the presence of these additional inputs, it is not clear whether it is valid to assume that motoneuron-burst neuron dynamics are negligable during saccades. A comprehensive analysis of the behavior of the motoneuron pool during saccadic eye movements, comparable to that performed on the burst neurons in this study, will be necessary in order to adequately address this issue.

Three questions arise regarding the burst generator organization: (1) How similar are the output characteristics of each cell group, and can they be lumped? (2) What are the delays in each line? (3) What does the discharge of one cell group contribute to the discharge of the target cell group or muscle? We submit that the objective evaluation of cell discharges and their latencies, as outlined in this article, can provide some answers to these questions.

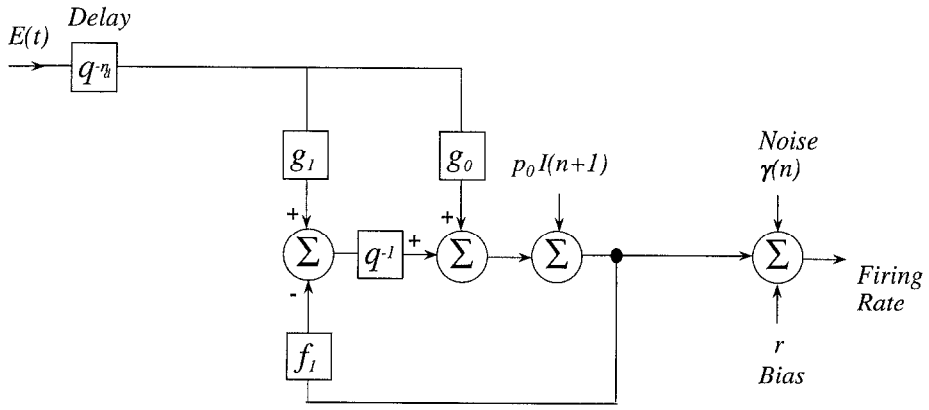

Figure 9. Diagram of the implementation of a system simulator for Eqs. (18) or (24) using a digital filter. In this illustration the filter uses two zeros and one pole. Observe that the noise $\gamma(n)$ is not fed back into the system simulator. For a multisaccadic system the filter has to be reinitialized for each saccade. Time zero makes reference to the filter reinitialization time.

Appendix

This appendix describes the methods used to estimate the parameters in the model formulated by Eq. (4), given eye position for input and firing rate estimate as output. Included here are the equations for the one-step-ahead predictors used to characterize the response of the saccadic system, when many saccades are averaged together as a population, and the algorithms we used for estimating the parameters. The Matlab System Identification Toolbox (SIT) provided a foundation for the algorithms we employed. We developed specialized algorithms that reinitialized the system response at the beginning of every saccade, and these are described in the section on the multisaccade predictor below. As shown in the main text, the "difference approximation" was employed in order to transform a continous-time model, such as that in Eq. (6), to a discrete-time representation.

The model structure used in this study, represented in terms of the shift operator q^{-1} is given by

$$B^k(n) = q^{-n_d}\frac{g(q)}{f(q)}E^k(n) + \frac{p^k(q)}{f(q)}I(n+nf) + r^k + \gamma(n), \qquad (24)$$

where

$$f(q) = 1 + f_1 q^{-1} + \cdots + f_{nf} q^{-nf} \qquad (25)$$

$$g(q) = g_0 + g_1 q^{-1} + \cdots + g_{ng-1} q^{-ng+1} \qquad (26)$$

$$p^k(q) = p_0^k + p_1^k q^{-1} + \cdots + p_{nf-1}^k q^{-nf+1} \qquad (27)$$

and n is within the interval that defines the kth saccade.

This more general form can be compared with Eq. (19) of the main text. The signal $I(n+nf)$ is a discrete impulse at time $n = -nf$ samples, q^{-1} is the shift operator. The integer nf refers to the number of poles, whereas ng refers to the number of elements in $g(q)$—the number of zeros + 1. The factor $p^k(q)$ is a representation of the initial state of saccade k; for $nf = 1$ (as was the case for the models tested here), the factor is a scalar. The term r^k indicates that the value of r may be estimated separately for each saccade, if desired.

The above model structure is called an output error (OE) formulation, in which the noise $\gamma(n)$ only appears at the output (Fig. 9). We consider in the Discussion the validity of choosing an OE formulation to represent burst neuron activity; an advantage of using this type of model structure is that it can generate unbiased estimates, even if the noise process is not white, so long as it has a zero mean (see Ljung, 1987, p. 75).

In models containing pole terms ($nf \geq 1$), there are initial conditions, and a single bias is assumed common to all saccades. If ns is the total number of saccades, the total number of parameters in such a model is the number of parameters in $g(q)$, $f(q)$, plus the parameters for the initial states and the bias.

$$P = nf + ng + ns * nf + 1. \qquad (28a)$$

In models in which there is no pole term ($nf = 0$), the bias is either:

(1) Estimated globally over all saccades, such that the number of parameters is the number of parameters

in $g(q)$ plus the bias.

$$P = ng + 1, \quad \text{or} \tag{28b}$$

(2) Estimated separately for each saccade, such that the number of parameters is the number of parameters in $g(q)$ plus the bias of each saccade:

$$P = ng + ns. \tag{28c}$$

The parameters in Eq. (24) are conveniently describe as the column vector θ.

$$\theta = [g_0, \ldots, g_{ng-1};\ f_1, \ldots, f_{nf};\ p_0^1, \ldots, p_{nf-1}^{ns};\ r]' \tag{29a}$$

$$\theta = [g_0, \ldots, g_{ng-1};\ r]' \tag{29b}$$

$$\theta = [g_0, \ldots, g_{ng-1};\ r^1, \ldots, r^{ns}]' \tag{29c}$$

for each of the model types described by Eqs. (28a), (28b), and (28c), respectively.

OE Multi-Saccade Predictor

The Matlab SIT is limited in that it allows building a model that fits only a single saccade, and furthermore the available modules are limited in that they do not account for the influence of a system's initial conditions on the output. Below, we summarize the considerations required for developing specialized algorithms that take account of initial condition when a model is fit to a population of saccades. For the case of a single saccade, an optimal one-step-ahead predictor of firing rate assuming the output error (OE) model in Eq. (24) is given by

$$\tilde{B}(n \mid n-1, \hat{\theta}) = q^{-\hat{n}_d}\frac{\hat{g}(q)}{\hat{f}(q)}E(n) + \frac{\hat{p}(q)}{\hat{f}(q)}I(n+nf) + \hat{r}, \tag{30}$$

where hat ($\wedge$) refers to parameter estimates, tilde ($\sim$) refers to the predictive estimate, and the expression $\tilde{B}(n \mid n-1, \hat{\theta})$ denotes the predicted firing rate $\tilde{B}(n)$ using the parameters set $\hat{\theta}$ estimated at time $n-1$.

In the models that contained pole terms, this recursive algorithm allows a prediction of the expected firing rate at the next sample time, given model parameters and current eye position. These parameters can be found by optimizing the fit over all the data points in the saccade using the modified OE algorithm. Recall that the noise and the initial conditions were added at the output side of the filter for such a model (Eq. (19) and Fig. 9).

Since the data we consider are composed of more than a single saccade, the predictor was generalized to multiple saccades, noting that $f(q)$, $g(q)$, and the bias are common to all saccades. To fit a model to more than one saccade, a multi-saccade OE one-step-ahead predictor is given by

$$\tilde{B}(n \mid n-1, \hat{\theta}) = w_z(n, \hat{\theta}) + w_\tau(n, \hat{\theta}), \tag{31}$$

where

$$w_z(n, \hat{\theta}) = q^{-\hat{n}_d}\frac{\hat{g}(q)}{\hat{f}(q)}E^k(n) + \hat{r}$$

$$w_\tau^k(n, \hat{\theta}) = \frac{\hat{p}^k(q)}{\hat{f}(q)}I\left(n + n_1^k + nf\right)$$

$$w_\tau(n, \hat{\theta}) = \sum_{k=1}^{ns} w_\tau^k(n)$$

and

- w_z is the response of the system assuming a zero initial state for the pole,
- w_τ^k is the transient response for saccade number, valid only for the length of the kth saccade,
- w_τ is the aggregate of the transient responses—that is, for any given n, only one term of this sum is non zero,
- n_1^k is the start sample time for the kth saccade.

The optimal predictor depended on the correct estimation of the delay n_d. In the analysis presented above (see Results), the value for n_d was obtained by finding a minimal cost for all estimated parameters, including n_d, using a simple but accurate model with no pole term (that is, $w_\tau = 0$ in Eq. (31)). To fit this model, dynamic linear regression equations were used (see below). Once estimated in this way, n_d was subsequently fixed in the multi-saccade predictor. The filter $g(q)/f(q)$ was restarted (the previous initial state was set to zero) before every saccade at $n = n_1^k - ng + 1$, where: ng is the number of zeros + 1, and time n_1^k is the first sample of the kth saccade. This differs from the assumption made in Rey and Galiana (1993), where filters were assumed to have a continuous response.

The residual of the predictor was defined as

$$v(n, \hat{\theta}) = B(n) - \tilde{B}(n \mid n-1, \hat{\theta}). \tag{32}$$

Note that the predictor was optimal within the stated model set if and only if the parameters in θ were known exactly—in this (unlikely) case, $v(n, \hat{\theta}) \equiv \gamma(n)$. The equations for the predictor are thus generally suboptimal depending on the correct estimate of the parameters in θ.

Algorithms Used for Estimating Parameters

The identification of a system is a two-step process. It involves first choosing the type and complexity of the model used to describe the system and second applying the correct algorithms to fit the parameters of the model. Most often, however, one must reassess the choice of the model and its complexity after comparing the errors of different competing models. This section describes the algorithms we used to compute parameters and to quantify the goodness of fit of the different models we proposed. Below are described the algorithms employed in the estimation of the two classes of models investigated in our analysis: (1) models in which there were no pole terms (regression algorithm) and (2) models in which there were pole terms (OE algorithm).

Regression Algorithm

If the model includes no poles ($f(q) \equiv 1$) then the predictor has no transient term. In this case parameters are estimated using the dynamic linear regression equations derived below. When the value of r is common to all saccades, the inputs of the system can be conveniently expressed by a $N \times d$ column vector. For example, consider a data set containing only two saccades (k_1 and k_2) which start at samples n_1^1, n_1^2 and end at samples n_{e1}^1, n_{e2}^2 of a sampled record, respectively. The input matrix ($\Phi(T_N)$) is given by

$$\Phi(T_N) = \begin{bmatrix} E(n_1^1) & \cdots & E(n_1^1 - ng + 1) & 1 \\ \vdots & & \vdots & \vdots \\ E(n_{e1}^1) & \cdots & E(n_{e1}^1 - ng + 1) & 1 \\ E(n_1^2) & \cdots & E(n_1^2 - ng + 1) & 1 \\ \vdots & & \vdots & \vdots \\ E(n_{e2}^2) & \cdots & E(n_{e2}^2 - ng + 1) & 1 \end{bmatrix}, \tag{33}$$

where

1. $T_N = (1, \ldots, N)$, an array of the relevant samples,
2. N is the number of elements in T_N,
3. ng is the number of elements in $g(q)$ (= number of zeros + 1), and
4. d represents the number of terms in the model. For example, in a model containing eye position, velocity, acceleration terms, and a bias term, $ng = 3$ and $d = 4$, such that the input matrix $\Phi(n) = |E(n)\ E(n-1)\ E(n-2)\ 1|$.

Similarly, the output ($B(T_N)$) is given by the $N \times 1$ column vector,

$$B(T_N) = \begin{bmatrix} B(1) \\ \vdots \\ B(N) \end{bmatrix}. \tag{34}$$

The criterion for estimating the parameters (θ), given by the column vector Eq. (29b), is to find the estimate that minimizes the following:

$$\begin{aligned} V(\theta) &= |B(T_N) - \Phi(T_N)\theta|^2 \\ &= [B(T_N) - \Phi(T_N)\theta]'[B(T_N) - \Phi(T_N)\theta], \end{aligned}$$

or equivalently, find the $\hat{\theta}$ such that

$$[\Phi'(T_N)\Phi(T_N)]\hat{\theta} = \Phi'(T_N)B(T_N). \tag{35}$$

Accordingly, the estimate of the parameters that minimizes the least squares criterion is

$$\hat{\theta} = [\Phi'(T_N)\Phi(T_N)]^{-1}\Phi'(T_N)B(T_N), \tag{36}$$

where, as noted above, the vectors do not define a single time interval but the aggregation of multiple saccade time intervals, such that all saccades are fit simultaneously.

In the case that r is estimated separately for each saccade, the column of ones in Eq. (33) is expanded into a k by N submatrix. For the example data set used in Eq. (33), that consisted of two saccades (k_1 and k_2) the input matrix $\Phi(T_N)$ would be given by

$$\Phi(T_N) = \begin{bmatrix} E(n_1^1) & \cdots & E(n_1^1 - ng + 1) & 1 & 0 \\ \vdots & & \vdots & \vdots & \vdots \\ E(n_{e1}^1) & \cdots & E(n_{e1}^1 - ng + 1) & 1 & 0 \\ E(n_1^2) & \cdots & E(n_1^2 - ng + 1) & 0 & 1 \\ \vdots & & \vdots & \vdots & \vdots \\ E(n_{e2}^2) & \cdots & E(n_{e2}^2 - ng + 1) & 0 & 1 \end{bmatrix}, \tag{37}$$

and the parameter column vector by Eq. (29c).

OE Algorithm

Models that include poles (such as Eqs. (4) and (6)) are complicated by the addition of transients. A damped Gauss-Newton type method based on that described by Ljung (1987, p. 284) is used to estimate system parameters for OE models. The method requires the computation of the gradients of the predictor, which are described by Eq. (38). The gradients are computed by taking partial derivatives of Eq. (31), with respect to each parameter:

$$\frac{\partial \tilde{B}(n)}{\partial \hat{g}_j} = q^{-n_d}\frac{1}{\hat{f}(q)}E^k(n-j) \tag{38a}$$

$$\frac{\partial \tilde{B}(n)}{\partial \hat{f}_j} = -\frac{1}{\hat{f}(q)}w_z(n-j) - \frac{1}{\hat{f}(q)}w_\tau(n-j) \tag{38b}$$

$$\frac{\partial \tilde{B}(n)}{\partial \hat{p}_j^k} = \frac{1}{\hat{f}(q)}I\left(n+n_1^k+nf-j\right) \tag{38c}$$

$$\frac{\partial \tilde{B}(n)}{\partial \hat{r}} = 1. \tag{38d}$$

where n is within the interval that defines the kth saccade.

The gradient matrix is obtained by stacking the gradients with respect to each parameter (including a vector of ones to represent the bias gradient):

$$\Delta = \left[\frac{\partial \tilde{B}}{\partial \hat{g}_0} \cdots \frac{\partial \tilde{B}}{\partial \hat{f}_1} \cdots \frac{\partial \tilde{B}}{\partial \hat{p}_0^1} \cdots \frac{\partial \tilde{B}}{\partial \hat{p}_{nf-1}^{ns}} \quad \vec{1}\right], \tag{39}$$

where Δ is stacked vertically as Φ was in Eq. (33) for the analysis of multiple saccades. The parameter column vector is defined as above Eq. (29a):

$$\theta = \left[g_0, \ldots, g_{ng-1};\ f_1, \ldots, f_{nf};\ p_0^1, \ldots, p_{nf-1}^{ns};\ r\right]'.$$

Damped Gauss-Newton Iterations

The criterion for determining the parameter estimate is to minimize the function

$$V(\theta) = \frac{1}{N}\sum_{n=1}^{N}(B_N - \tilde{B}_N)^2. \tag{40}$$

For a given iteration, the time varying residual (error) of the predictor is defined as:

$$v(n, \hat{\theta}) = B(n) - \tilde{B}(n \mid n-1, \hat{\theta}). \tag{32}$$

The error is first determined for a given parameter set, and then the parameter estimate is "updated" iteratively. This is done according to

$$\theta^{(i+1)} = \theta^{(i)} + \mu h^{(i)}, \tag{41}$$

where μ is a positive constant that corresponds to the iteration step size, and h represents a function that is determined based on values of the $v(n, \hat{\theta})$, its gradient, and of its Hessian (the second derivative matrix) and the index i makes reference to the ith approximation (iteration) of the system parameters.

The general form of the damped Gauss-Newton iterative algorithm is

$$\theta^{(i+1)} = \theta^{(i)} + \mu^{(i)}\left[\Delta^{(i)'}\Delta^{(i)}\right]^{-1}\Delta^{(i)'}v^{(i)}, \tag{42}$$

where

1. μ is the step size $0 < \mu \leq 1$ (the algorithm is called *damped* when $\mu < 1$),
2. Δ is the gradient matrix, and
3. $\Delta^{(i)'}\Delta^{(i)}$ is the Gauss-Newton approximation of the Hessian.

The algorithm consists of three steps:

1. Compute the gradient according to Eqs. (38) and (39).
2. Compute the new parameters from previous estimates Eq. (42) using a unity step.
3. Halve step size up to 10 times to attempt to reduce the error. If error is not reduced or error acceptably small exit, otherwise go back to Step 1.

A measure of robustness is achieved by eliminating outliers from the estimated residuals (Ljung, 1987, p. 401; Devore, 1982; Rey, 1992).

Initial Conditions Taken from Data

There are two methods for fitting initial conditions to data. The method above includes fitting the transients in the optimization process. However, this method is calculation intensive and therefore can be very time consuming. Another approach taken by Ljung (1987, p. 308) is to use the startup data to approximate the initial conditions for each saccade interval. This method is based on a finite memory implementation of Eq. (24),

which can be rewritten as

$$f(q)B^k(n) = g(q)E^k(n) + p^k(q)I(n+nf) + f(q)r^k + f(q)\gamma(n).$$

Then

$$p^k(q)I(n+nf) = f(q)B^k(n) - g(q)E^k(n) - f(q)r^k - f(q)\gamma(n).$$

Thus an estimate of the initial conditions for the kth saccade is

$$\hat{p}^k(q)I(n+nf) = \hat{f}(q)(B^k(n) - \hat{r}^k) - \hat{g}(q)E(n), \tag{43}$$

where the previous estimates, $\hat{g}(q)$, $\hat{f}(q)$, and $\hat{r}^k$ are used to estimate $\hat{p}^k$.

Using the initial firing rate to estimate the transient component reduces the number of parameters from $P = (nf + ng + ns * nf + 1)$ to $P = (nf + ng + 1)$. The number of calculations required in this method are greatly reduced from that described in the preceding sections (in which the transients are fit in the optimization), thereby significantly reducing the time required to complete a computation. On the other hand, the burst neuron firing rate near the beginning of a burst is most likely to depend on the time course of the release of inhibitory inputs (Fuchs et al., 1985), and therefore its values may be quite noisy; furthermore the influence of the first few spikes on the output may be limited due to the necessity of depolarizing motoneuron membranes. In a subsequent report that will included our entire data set, we will consider the relative usefulness of these two methods regarding the characterization of burst neuron spike trains.

Acknowledgment

This study was supported by the Medical Research Council of Canada (MRC), the U.S. National Institutes of Health (NIH) and the Human Frontiers Science Organization.

References

Baker R, Evinger R, McCrea RA (1981) Some thoughts about the three neurons in the vestibulo-ocular reflex. *Ann. NY Acad. Sci.* 374:171–188.

Caines PE (1988) Linear Stochastic Systems. John Wiley & Sons, Toronto.

Cannon SC, Robinson DA (1987) Loss of the neural integrator of the oculomotor system from brain stem lesions in monkey. *J. Neurophysiol.* 57:138–146.

Cheron G, Godaux E (1987) Disabling of the oculomotor neural integrator by kainic acid injections in the prepositus-vestibular complex of the cat. *J. Physiol. Lond.* 394:267–290.

Cheron G, Gilles P, Godaux E (1986a) Lesions in the cat prepositus-vestibular complex: Effects on the optokinetic system. *J. Physiol. Lond.* 372:95–111.

Cheron G, Godaux E, Laune JM, Vanderkelen B (1986b) Lesions in the cat prepositus-vestibular complex: Effects on the vestibular ocular reflex and saccades. *J. Physiol. Lond.* 372:75–94.

Cullen KE, McCrea RA (1993) Firing behavior of brainstem neurons during voluntary cancellation of the horizontal vestibulo-ocular reflex. I. Secondary vestibular neurons. *J. Neurophysiol.* 70:828–855.

Cullen KE, Chen-Huang C, McCrea RA (1993) Firing behavior of brainstem neurons during voluntary cancellation of the horizontal vestibulo-ocular reflex. II. Eye movement related neurons. *J. Neurophysiol.* 70:844–856.

Devore JL (1982) Probability and Statistics for Engineering and the Sciences. Brooks/Cole, Monterey, CAL.

Escudero M, De La Cruz RR, Delgado-Garcia JM (1992) A comparative neurophysiological study of prepositus hypoglossi and vestibular neurons projecting to the abducens nucleus in the alert cat. *J. Physiol. Lond.* 458:539–560.

Fuchs AF, Kaneko CRS, Scudder CA (1985) Brainstem control of saccadic eye movements. *Ann. Rev. Neuroscience* 8:307–337.

Fuchs AF, Scudder CA, Kaneko CRS (1988) Discharge patterns and recruitment order of identified motor neurons and internuclear neurons in the monkey abducens nuclei. *J. Neurophysiol.* 60:1874–1895.

Galiana HL, Guitton D (1992) Central organization and modeling of eye-head coordination during orienting gaze shifts. In: B Cohen, DL Tomko, F Guedry, eds. Sensing and Controlling Motion. New York Academy of Sciences, New York. pp. 452–471.

Goldstein HP, Robinson DA (1984) A two-element oculomotor plant model solves problems inherent in a single-element plant model. *Soc. Neurosci. Abstr.* 10:909.

Grantyn A, Bertoz A (1985) Burst activity of identified tecto-reticulospinal neurons in the alert cat. *Exp. Brain Res.* 57:417–421.

Guitton D, Douglas RM, Volle M (1984) Eye-head coordination in cats. *J. Neurophysiol.* 52:427–459.

Harris CM, Wallman J, Scudder CA (1990) Fourier analysis of saccades in monkeys and humans. *J. Neurophysiol.* 63:877–886.

Hepp K, Henn V, Vilis T, Cohen B (1989) Brainstem regions related to saccade generation. In: RH Wurtz, ME Goldberg, eds. The Neurobiology of Saccadic Eye Movement. Elsevier North-Holland, Amsterdam. pp. 105–211.

Hikosaka O, Kawakami T (1977) Inhibitory neurons related to the quick phase of vestibular nystagmus their location and projection. *Exp. Brain Res.* 27:377–396.

Hikosaka O, Igusa Y, Nakao S, Shimazu H (1978) Direct inhibitory synaptic linkage of pontomedullary reticular burst neurons with abducens motoneurons in the cat. *Exp. Brain Res.* 33:337–352.

Igusa Y, Sasaki S, Shimazu H (1980) Excitatory premotor burst neurons in the cat pontine reticular formation related to the quick phase of vestibular nystagmus. *Brain Res.* 182:451–456.

Johansen TA, Foss BA (1993) Constructing NARMAX models using ARMAX models. *Intl. J. of Control.* 58:1125.

Jurgens R, Becker W, Kornhuber H (1981) Natural and drug-induced variations of velocity and duration of human saccadic eye movements: Evidence for the neural pulse generator by local feedback. *Biol. Cybern.* 39:87–96.

Kaneko CRS, Fuchs AF (1981) Inhibitory burst neurons in alert trained cats: Comparison with excitatory burst neurons and functional implications. In: AF Fuchs, W Becker, eds. Progress in Oculomotor Research. Elsevier North-Holland, Amsterdam. pp. 63–70.

Keller EL (1973) Accommodative vergence in the alert monkey: Motor unit analysis. *Vision Res.* 13:1565–1575.

Kuo BC (1992) Digital Control Systems. Saunders College Publishing, Orlando FL.

Ljung L (1987). System Identification: Theory for the User. Prentice-Hall, Englewood Cliffs, NJ.

Lopez-Barneo J, Darlot C, Bertoz A, Baker R (1982) Neural activity in prepositus nucleus correlated with eye movements in the alert cat. *J. Neurophysiol.* 47:329–352.

Mathworks Inc. (1987) System Identification Toolbox. Natick Massachussettes. Copyright by the Mathworks.

McFarland JL, Fuchs AF (1992) Discharge patterns of nucleus prepositus hypoglossi and adjacent vestibular nucleus during horizontal eye movement in behaving macaques. *J. Neurophysiol.* 68:319–332.

Mettens P, Godaux E, Cheron G, Galiana HL (1994) Effect of Muscimol microinjections into the prepositus hypoglossi and medial vestibular nuclei on cat eye movements. *J. Neurophysiol.* 72:785–802.

Munoz DP, Guitton D, Pelisson D (1991) Control of orienting gaze shifts by the tectoreticulospinal system in the head-free cat. III. Spatiotemporal characteristics of phasic motor discharges. *J. Neurophysiol.* 66:1642–1666.

Optican LM, Miles FA (1985) Visually induced adaptive changes in primate saccadic oculomotor control signals. *J. Neurophysiol.* 54:940–958.

Pare M, Guitton D (1990) Gaze-related activity of brainstem omnipause neurons during combined eye-head gaze shifts in the alert cat. *Exp. Brain Res.* 83:210–214.

Pintelon R, Kollar I (1991) Exact discrete time representation of continuous time systems. *Proceedings 9th IFAC/IFORS Symposium in Identification and System Parameter Estimation*, pp. 1628–1633.

Rey CG (1992) New algorithms for the classification and identification of the vestibulo-ocular reflex. Ph.D. Thesis, McGill University.

Rey CG, Galiana HL (1993) Transient analysis of vestibular nystagmus. *Biol. Cybern.* 69:395–405.

Richmond BJ, Optican LM, Podell M, Spitzer H (1987) Temporal encoding of two-dimensional patterns by single units in primate inferior temporal cortex. I. Response characteristics. *J. Neurophysiol.* 57:132–146.

Robinson DA (1964) The mechanics of human saccadic eye movement. *J. Physiol. Lond.* 174:245–264.

Robinson DA (1970) Oculomotor unit behavior in the monkey. *J. Neurophysiol.* 33:393–404.

Robinson DA (1975) Oculomotor control signals. In: G Lennerstrand, P Bach-y-Rita, eds. Basic Mechanisms of Ocular Motility and their Clinical Implications. Pergamon, Oxford. pp. 337–374.

Sales KR, Billings SA (1990) Self-tuning control of non-linear ARMAX models. *Intl. J. of Control.* 51:753.

Sanderson AC, Kobler B (1976) Sequential interval histogram analysis of non-stationary neural spike trains. *Biol. Cybern.* 22:61–71.

Sasaki S, Shimazu H (1981) Reticulovestibular organization participating in the generation of horizontal fast eye movement. *Ann. NY Acad. Sci.* 374:130–143.

Schwarz G (1978) Estimating the dimension of a model. *Ann. Statist.* 6:461–464.

Scudder CA (1988) A new local feedback model of the saccadic burst generator. *J. Neurophysiol.* 59:1455–1475.

Scudder CA, Fuchs AF (1992) Physiological and behavioral indentification of vestibular nucleus neurons mediating the horizontal vestibuloocular reflex in trained Rhesus monkeys. *J. Neurophysiol.* 69:244–264.

Scudder CA, Fuchs AF, Langer TP (1988) Characteristics and functional identification of saccadic inhibitory burst neurons in the alert monkey. *J. Neurophysiol.* 59:1430–1454.

Silverman BW (1986) Density Estimation for Statistics and Data Analysis. Chapman and Hall, London.

Strassman A, Highstein SM, McCrea RA (1986a) Anatomy and physiology of saccadic burst neurons in the alert Squirrel monkey. I. Excitatory burst neurons. *J. Comp. Neurol.* 249:337–357.

Strassman A, Highstein SM, McCrea RA (1986b) Anatomy and physiology of saccadic burst neurons in the alert Squirrel monkey. II. Inhibitory burst neurons. *J. Comp. Neurol.* 249:358–380.

Van Gisbergen JAM, Robinson DA, Gielen S (1981), A quantitative analysis of generation of saccadic eye movements by burst neurons. *J. Neurophysiol.* 45:417–442.

Van Opstal AJ, Van Gisbergen JAM, Eggermont JJ (1985) Reconstruction of neural control signals for saccades based on and inverse method. *Vision Res.* 25:789–801.

Vijayan R, Poor HV, Moore JB, Goodwin GC (1991) A Levinson type algorithm for modeling fast sampled data. *IEEE Trans. on Automatic Control.* 36(3):314–321.

Yoshida K, Berthoz A, Vidal PP, McCrea RA (1982) Morphological and physiological characteristics of inhibitory burst neurons controlling rapid eye movements on the alert cat. *J. Neurophysiol.* 48:761–784.

Zellner A (1984) Posterior odds ratios for regression hypotheses: General implications and some specific results. In: Basic Issues in Econometrics. University of Chicago Press, Chicago. pp. 275–305.

Zuber BL, Semmlow JL, Stark L (1968) Frequency characteristics of the saccadic eye movement. *Biophysical J.* 8:1288–1298.